Solvation Structure of Poly(ethylene glycol) in Ionic Liquids Studied by High-energy X-ray Diffraction and Molecular Dynamics Simulations

ARTICLE *in* MACROMOLECULES · MARCH 2013

Impact Factor: 5.8 · DOI: 10.1021/ma400218e

7 AUTHORS, INCLUDING:

Kenta Fujii
Yamaguchi University
83 PUBLICATIONS **1,758** CITATIONS
SEE PROFILE

Takamasa Sakai
The University of Tokyo
93 PUBLICATIONS **1,539** CITATIONS
SEE PROFILE

Koji Ohara
Kyoto University
37 PUBLICATIONS **118** CITATIONS
SEE PROFILE

Mitsuhiro Shibayama
The University of Tokyo
317 PUBLICATIONS **8,706** CITATIONS
SEE PROFILE

Macromolecules

Article

pubs.acs.org/Macromolecules

Solvation Structure of Poly(ethylene glycol) in Ionic Liquids Studied by High-energy X-ray Diffraction and Molecular Dynamics Simulations

Hanako Asai,[†] Kenta Fujii,[†,*] Kengo Nishi,[†] Takamasa Sakai,[‡] Koji Ohara,[§] Yasuhiro Umebayashi,[⊥] and Mitsuhiro Shibayama[†,*]

[†]Institute for Solid State Physics, The University of Tokyo, 5-1-5 Kashiwanoha, Kashiwa, Chiba 277-8581, Japan.

[‡]Department of Bioengineering, School of Engineering, The University of Tokyo, 7-3-1 Hongo, Bunkyo-ku, Tokyo 113-8656, Japan

[§]Japan Synchrotron Radiation Institute (JASRI), Sayo-cho, Sayo-gun, Hyogo, 679-5198, Japan.

[⊥]Graduate School of Science and Technology, Niigata University, 8050, Ikarashi, 2-no-cho, Nishi-ku, Niigata City, 950-2181, Japan

Supporting Information

ABSTRACT: Solvation structures of poly(ethylene glycol) (PEG) in 1-ethyl-3-methylimidazolium-based ionic liquids solution were studied by using high-energy X-ray diffraction (HEXRD) and molecular dynamics (MD) simulation in terms of dependences on the anion-type for ILs, molecular weight (M_w), concentration and shape (linear or tetra-armed) for PEG. It was found from HEXRD experiment that there is no M_w and shape dependences for PEG in 1-ethyl-3-methylimidazolium bis(trifluoromethansulfonyl)amide, [C_2mIm$^+$][TFSA$^-$] solution, implying that the local structure (r < 15 Å) is not influenced by M_w and shape of PEG. From the HEXRD results with the aid of MD simulations, it was found that C_2mIm cation preferentially solvates to PEG in all the ILs, and TFSA is distributed randomly with van der Waals and weak electrostatic interactions. The atom−atom pair correlation and space distribution functions evaluated from the MD simulations revealed that hydrogen bonding interactions are formed between C2 carbon within the imidazolium ring and O (PEG), which is essentially different from C4 carbon−O and C5 carbon−O interactions. Finally, we discussed the relationship between the obtained microscopic solvation structures and the macroscopic properties of PEG-based gel (swelling ratio and χ parameters).

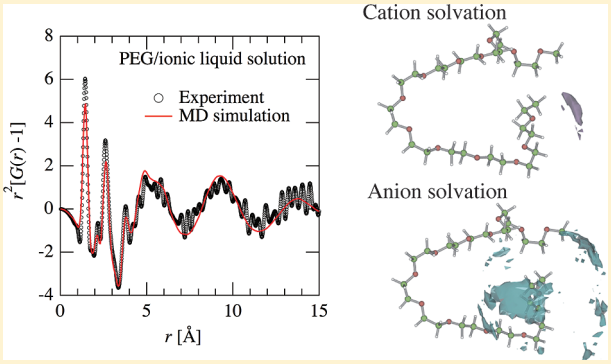

1. INTRODUCTION

Room temperature ionic liquids (ILs) consist only of ions and thus the solvent properties essentially differ from water and/or conventional organic solvents.[1] Because ILs possess characteristic properties such as nonvolatility, nonflammability, high ionic conductivity, it has been expected as new solvents for many fields such as electrochemistry,[2−4] organic chemistry,[5] catalysis chemistry,[6] and soft matter science.[7]

In soft matter field, typical aprotic ILs such as 1-alkyl-3-methylimidazolium-, *N*-alkylpyrrolydinium-, and *N*,*N*-pyrazonium-based ILs can easily dissolve polymers, and the solubility is often controlled by anion species in IL rather than cation ones. Rogers et al. reported for the first time that 1-butyl-3-methylimidazolium chloride, [C_4mIm$^+$][Cl$^-$] can dissolve cellulose, which is insoluble in conventional solvents because of its many intramolecular hydrogen bonds, by heating only at 100 °C and the solubility strongly depends on the anion species.[8] Recently, Ohno et al. have reported a series of alkylimidazolium ILs composed of phosphonate- and phosphinate-based anion, which show a high solubility of cellulose under mild condition.[9,10] Interestingly, 1-ethyl-3-methylimidazolium methylphosphonate can dissolve 2−4 wt % cellulose at room temperature and 10 wt % at 45 °C. These indicate that the interaction between cellulose and IL anion plays a key role on dissolution of cellulose to disrupt the intramolecular hydrogen bonds within cellulose, which is applied to all the polymer/IL solution systems. Tsuda et al. reported ^{1}H NMR chemical shifts for poly(ethylene glycol) (PEG) derivatives in 1-ethyl-3-methylimidazolium bis(trifluoromethanesulfonyl)-amide ([C_2mIm$^+$][TFSA$^-$]) solution, and pointed out that hydrogen bonds are formed between the oxygen of PEG derivatives and the proton within the imidazolium ring (C_2mIm$^+$).[11] Lodge et al. reported a lower critical solution temperature (LCST)-type phase separation of PEG derivatives in [C_2mIm$^+$][BF_4^-] and its analogous IL.[12] They proposed that the phase behaviors strongly depends on the PEG−C_2mIm

Received: January 31, 2013
Revised: March 1, 2013
Published: March 15, 2013

   dx.doi.org/10.1021/ma400218e | *Macromolecules* 2013, 46, 2369−2375

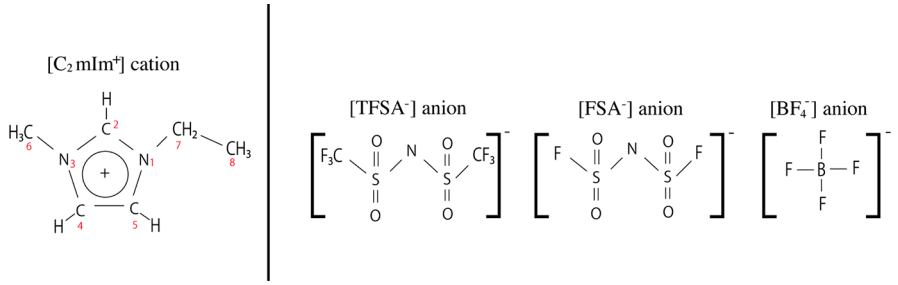

Figure 1. Schematic structure cation and anions used in this study. The atoms of the cation are numbered in red.

interactions at the molecular level, particularly, hydrogen bonding between them, and then the microscopic images of the interactions are described as schematic illustrations (Figures 3 and 4 in ref 12) based on above NMR results. The PEG−IL interactions were also investigated by molecular dynamics (MD) simulations.[13] However, direct experimental evidence for the polymer solvation have never been reported yet at the present stage. Here, note that the combination of X-ray/neutron diffraction with MD simulations is a powerful method to perform direct determination of the microscopic solvation structure, i.e., distance, orientation, and coordination number for the intermolecular interactions between solute and solvent, and then the obtained results are obviously based on both of experimental and theoretical evidence. Indeed, we recently demonstrated a high-energy X-ray diffraction (HEXRD) experiment with the aid of MD simulations on benzyl methacrylate in IL solution system to reveal the solvation structure. It was clearly found that benzyl group of benzyl methacrylate is preferentially solvated by [C_2mIm$^+$] cation, and the specific solvation leads to a lower-critical-solution-temperature- (LCST-) type phase separation of the corresponding polymer solutions (poly(benzyl methacrylate) in IL solutions).[14,15]

An ion gel has been focused on the applications to actuators,[16,17] electrolytes,[4] CO_2 separation membranes,[18] and so on, and the mechanical and structural properties of ion gel are strongly related to the corresponding solution system. Recently, it has been established in our recent study that tetra-arm poly(ethylene glycol) (Tetra-PEG) ion gel, which can be prepared by A-B type cross-end coupling of two symmetrical tetra-arm PEG macromers in IL, shows high mechanical and ion-conducting properties even at low polymer concentration.[19] The Tetra-PEG ion-gel has studied by using small-angle neutron scattering (SANS)[20] to elucidate nanoscale structure, suggesting that the high mechanical properties of the Tetra-PEG ion gel are strongly related to homogeneous polymer network structure in the gel. Furthermore, we have also investigated the gelation process of the ion gel by time-resolved dynamic light scattering (TR-DLS) measurement.[21] Through our systematic study on Tetra-PEG ion gel, we pointed out that the reaction efficiency is different between ionic liquid and aqueous solution systems. It is expected that dissolved state of polymer molecules before the gelation, i.e., shrinking or expanding of polymer in the solution, and their solvation at local scale play a key role on the gelation reaction. According to our SANS study, [C_2mIm$^+$][TFSA$^-$] acts as a good solvent for Tetra-PEG, however, knowledge of the local solvation structure of PEG (hydrogen bond, van der Waals interaction, charge−charge interaction) in IL is still limited at the present stage. It is difficult to quantitatively analyze the solvation structure of polymer with large molecular weight, because the Tetra-PEG exists as a complicated state in solution.

In this work, we carried out HEXRD measurements on the PEG/[C_2mIm$^+$][TFSA$^-$] solutions with various molecular weight and shape (linear or tetra-armed) to elucidate the solvation of PEG. In order to obtain more insight into the solvation in IL system, in addition, we performed MD simulations for linear PEG with relatively small molecular weight as a model molecule of the PEG/[C_2mIm$^+$][TFSA$^-$] solutions. By applying the HEXRD with the aid of MD simulations to the present polymer solution system, we clearly showed the distance, orientation, and coordination number on the solvation of PEG, and their IL anion dependences were discussed in detail on the basis of radial distribution function at microscopic level (r < 15 Å). Furthermore, we compared the results with those of swelling measurements of the PEG-based gels prepared in the ILs and pointed out a certain correlation between the microscopic structure and macroscopic swelling properties. It seems that the findings obtained from both micro- and macroscopic experiments are important in the field of polymer science.

2. EXPERIMENTAL SECTION

2.1. Samples. We used 1-ethyl-3-methylimidazolium cation ([C_2mIm$^+$])-based ILs with three different anions; bis(trifluoromethanesulfonyl)amide ([TFSA$^-$]), bis(fluorosulfonyl)amide ([FSA$^-$]), and tetrafluoroborate ([BF_4^-]) in this work and their chemical structures are shown in Figure 1. For [C_2mIm$^+$][TFSA$^-$] solution systems, the concentration of PEG (600 g/mol) was varied from 10 up to 30 wt %, and M_w for PEG was varied from 600, 2000, and 4600 g/mol at the fixed PEG concentration (20 wt %). For [C_2mIm$^+$][FSA$^-$] and [C_2mIm$^+$][BF_4^-] solution systems, the concentration and M_w for PEG were fixed at 30 wt % and 600 g/mol, respectively.

[C_2mIm$^+$][TFSA$^-$] was synthesized according to the previous report.[1,22,23] [C_2mIm$^+$][FSA$^-$] and [C_2mIm$^+$][BF_4^-] were purchased from Piotrek Co. Ltd. and Kanto Chemical Co. Inc., respectively. These ILs were dried under vacuum. The water contents were checked by Karl Fischer titration to be less than 100 ppm. PEGs were purchased from Wako chemical Co. Ltd. (600 g/mol) and Sigma-Aldrich Co. Ltd. (2000 g/mol and 4600 g/mol), respectively. Tetra-amine-terminated PEG (TAPEG) (M_w = 10 kg/mol) was provided from Nichiyu, Co. Ltd.

2.2. Swelling Ratio Measurement. The swelling ratio (Q) measurements were carried out for completely dried 10 kg/mol 50 mg/mL Tetra-PEG hydrogels prepared in capillaries. The dried Tetra-PEG gels were immersed in each IL for 24 h at 25 °C thermostat bath. The Q values were defined as a change of diameters between the dry state (d_{dry}) and swelling equilibrium state ($d_{swollen}$); $Q = (d_{swollen}/d_{dry})^3$.

2.3. HEXRD Measurements. HEXRD measurements were performed at room temperature by using high-energy X-ray diffraction apparatus of BL04B2 beamline at SPring-8 (Japan Synchrotron Radiation Research Institute, JASRI, Japan).[24,25] The samples were set in a flat cell (2 mm thickness) consisting of poly(ether−ether-ketone)

dx.doi.org/10.1021/ma400218e | Macromolecules 2013, 46, 2369−2375

plate as a body covered with Kapton films as an X-ray window, hermetically sealed with Kalrez O-rings, and stainless steel cover plates. Monochrome 61.6 keV X-rays were obtained using a Si(220) monochromator. The exposure time for each sample was about 4.5 h. The observed X-ray intensity was corrected for absorption[26] and polarization. Incoherent scatterings were subtracted from the observed scatterings to obtain the $I_{coh}(q)$.[27−29] The X-ray structure factor $S^{exp}(q)$ and X-ray radial distribution function $G^{exp}(r)$ per stoichiometric volume were obtained as follows:

$$S^{exp}(q) = \frac{I_{coh}(q) - \sum n_i f_i(q)^2}{(\sum n_i f_i(q))^2} + 1 \quad (1)$$

$$G^{exp}(r) - 1 = \frac{1}{2\pi^2 r \rho_0} \int_0^{q_{max}} q\{S(q) - 1\} \sin(qr) \exp(-Bq^2)\, dq \quad (2)$$

where n_i and $f_i(q)$ are the number and atomic scattering factor of atom i,[30] respectively, ρ_0 is the number density, and B is the damping factor.

2.4. MD Simulations. An MD simulation for an *NTP* ensemble (298 K and 1 atm) in a cubic cell was carried out using Materials Explorer 4.0 program (Fujitsu), and the composition (number of ion-pair and PEG) in a given system is listed in Table S1, Supporting Information. The simulation time was 2 ns for all the systems. The system was equilibrated for the first 1.5 ns with an interval of 0.2 fs, and the data collected at every 0.2 fs during 1.5−2 ns were used to extract the structure factors and the radial distribution function. CLaP and OPLS-AA force fields were used for IL ions and PEG, respectively,[31−33] including intermolecular Lennard-Jones and Coulombic interactions, and intramolecular interactions with bond stretching, angle bending, and torsion of dihedral angles.[33] The detail procedure has been described elsewhere.[34−40] Density values obtained by the MD simulations are in good agreement with the corresponding experimental ones, which is also listed in Table S1, Supporting Information.

The X-ray structure factor $S^{MD}(q)$ was calculated as follow:

$$\begin{cases} S^{MD}(q) = \dfrac{\sum_i \sum_j \{n_i(n_j - 1) f_i(q) f_j(q)/N(N-1)\}}{\{\sum_k (n_k f_k(q)/N\}^2} \times \int_0^r 4\pi r^2 \rho_0 (g_{ij}^{MD}(r) - 1) \dfrac{\sin(qr)}{qr} dr + 1 & (i = j) \\ S^{MD}(q) = \dfrac{\sum_i \sum_j (2 n_i n_j f_i(q) f_j(q)/N^2)}{\{\sum_k (n_k f_k(q)/N\}^2} \times \int_0^r 4\pi r^2 \rho_0 (g_{ij}^{MD}(r) - 1) \dfrac{\sin(qr)}{qr} dr + 1 & (i \neq j) \end{cases} \quad (3)$$

where ρ_0 means the ensemble average of the number density. The total number of atoms in the simulation box N is given by

$$N = \sum_k n_k \quad (4)$$

The X-ray radial distribution function $G^{MD}(r)$ was obtained from $S^{MD}(q)$ by a Fourier transform procedure similar to that of $S^{exp}(q)$.

3. RESULTS AND DISCUSSION

3.1. Swelling Ratio and χ Parameter of PEG/IL Systems. At first, we carried out the swelling ratio measurements, where the completely dried Tetra-PEG hydrogels were swollen by the ILs, and calculated the polymer−solvent interaction parameter, i.e. χ parameters, for each IL/PEG system via following Flory−Rehner's equation.[41]

$$\nu = \frac{\{\ln(1-\phi) + \phi + \chi\phi^2\}}{V_1\left(\frac{1}{2}\phi - \phi^{1/3}\right)} \quad (5)$$

Here, ν is the cross-linking density, which has already determined in our previous paper[42] and ϕ is the polymer volume fraction at equilibrium swelling, which was obtained by the swelling ratio, Q. The V_1 value is the molar volume of the solvent. By substituting ν, ϕ, and V_1 into eq 5, χ parameter for each IL/PEG system was obtained and the data were summarized in Table 1. As shown in this table, the Q values

Table 1. Swelling Ratio (Q) and the χ Parameter for Each IL/PEG System

	Q [−]	χ [−]
TFSA system	13	0.43
FSA system	9.4	0.48
BF_4 system	1.1	–

decreased in the order of $[TFSA^-]$ > $[FSA^-]$ > $[BF_4^-]$ system. The solvent $[C_2mIm^+][BF_4^-]$ hardly swelled the dried Tetra-PEG gel, and we thus could not estimate the Q value in this system. In the Flory−Huggins lattice theory, an interaction parameter, χ, is defined as a nondimensionalizationed difference of contact energy between solvent and polymer, and it is used as an indication of the solubility of polymer:[43] As the χ parameter approaches to 0.5, a solubility of a polymer becomes lower. However, there are no insights about between the χ parameter (or the solubility) and the solvation structure in polymer solutions. We thus investigated the solvation structure of PEG in IL solution at the atomistic level by using HEXRD and MD simulations, and discussed the relationship between the macroscopic (swelling ratio and χ parameter) and the structural microscopic properties.

3.2. HEXRD. Figure 2a shows the observed $S^{exp}(q)$ for 600 g/mol PEG in $[C_2mIm^+][TFSA^-]$ solutions in the q-range of

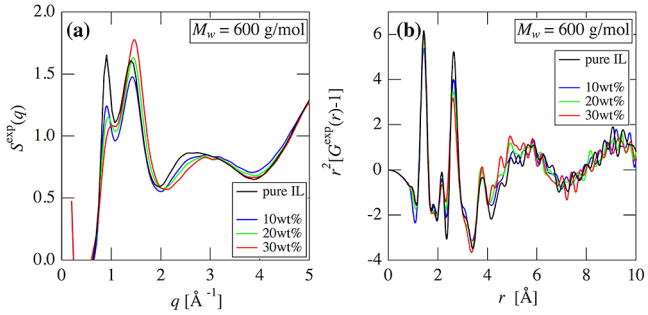

Figure 2. PEG concentration dependence of (a) $S^{exp}(q)$s and (b) $r^2[G^{exp}(r) - 1]$s for PEG/$[C_2mIm^+][TFSA^-]$ solutions in the q-range of 0.15−5 Å^{-1} and the r-range of 0−10 Å, respectively.

0.15−5 Å^{-1}, together with the corresponding neat $[C_2mIm^+][TFSA^-]$.[44] The $S^{exp}(q)$ at the whole q-range examined here (~22 Å^{-1}) is shown in Figure S1, Supporting Information. The intensity in the first peak at 0.9 Å was weakened with increasing the PEG concentration and the reverse was observed in the second one at 1.5 Å. This indicates that intermolecular interaction between PEG and IL ions (cation and anion) is formed and then ion−ion interaction of $[C_2mIm^+][TFSA^-]$ is broken in the solution. The M_w dependence on the $S^{exp}(q)$ for 20 wt % PEG/$[C_2mIm^+][TFSA^-]$ solutions is shown in Figure

dx.doi.org/10.1021/ma400218e | Macromolecules 2013, 46, 2369−2375

S2, Supporting Information. As shown in this figure, a clear M_w difference was not observed in the $S^{exp}(q)$ in the range of q = 0.15−22 Å^{-1}, although significant M_w dependence was observed by previous SANS study (q = 0.003−0.3 Å^{-1}).[20] In general, $S^{exp}(q)$ in the former q-range reflects a structure at molecular or atomistic scale (∼ Å scale), while that in the latter is over a nanoscale. It is thus implied that no M_w and shape dependences on the local solvation structure of PEG in the TFSA-based IL solutions are observed from the HEXRD, which is an assumption as a first step in this work. We thus carried out MD simulation for the smallest M_w (600 g/mol) PEG in IL solutions with different anions ([TFSA$^-$], [FSA$^-$], and [BF$_4^-$]) and PEG concentrations to discuss the solvation structure of PEG in these ILs, as mentioned in a latter section.

Figure 2b shows the experimental radial distribution function, $G^{exp}(r)$ as a form of $r^2[G(r) - 1]$ for 600 g/mol PEG in [C$_2$mIm$^+$][TFSA$^-$] solutions in the r-range of 0−10 Å, together with the corresponding neat [C$_2$mIm$^+$][TFSA$^-$].[44] The $G^{exp}(r)$ in the whole r-range (0−22 Å) is shown in Figure S1, Supporting Information. It has been established in our previous works that the peaks at r < 3 Å is mainly assigned to the intramolecular interactions for solute and solvent.[44] In the r-range of 3−6 Å, the component for intermolecular interaction is seriously overlapped with that for the intramolecular interaction.[23,37] Therefore, we tried to extract a partial radial distribution function for intermolecular component, particularly, PEG-IL interaction, from the total $G^{MD}(r)$ to discuss solvation of PEG in IL solution.

3.3. MD Simulations. Figure 3 shows typical result for X-ray-weighted radial distribution function, $r^2[G(r) - 1]$s for 30

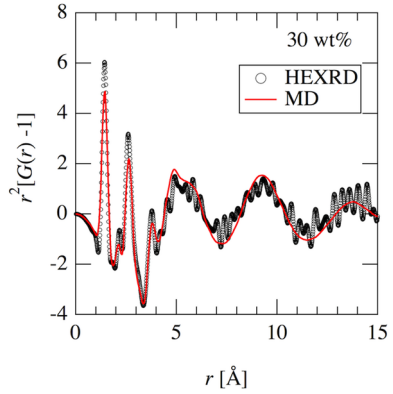

Figure 3. X-ray-weighted $G(r)$ for 30 wt % PEG/[C$_2$mIm$^+$][TFSA$^-$] obtained from HEXRD experiment (open circle) and MD simulation (solid line).

wt % PEG (600 g/mol) in [C$_2$mIm$^+$][TFSA$^-$] solution, obtained from the MD simulation (solid line), together with the corresponding HEXRD one (circled). It can be seen that the HEXRD result is well reproduced by MD simulations, indicating the validity of MD results in this work. This correspondence also can be seen for the other systems with various concentrations and anions.

The total radial distribution function, $G^{MD}(r)$ can be deconvoluted into intra- and intermolecular components, $G^{MD}_{intra}(r)$ and $G^{MD}_{inter}(r)$, which are shown in Figure S3, Supporting Information. The total intermolecular $G^{MD}(r)$ is composed of six intermolecular interactions, i.e., PEG−cation, PEG−anion, PEG−PEG, cation−cation, anion−anion, and cation−anion. To elucidate the solvation structure of PEG in detail, the partial radial distribution functions for their intermolecular interactions were extracted from the $G^{MD}_{inter}(r)$, and typical results with regard to solvation of PEG are shown in Figure 4. It was found that the $G^{MD}_{PEG\text{-}cat}(r)$ for PEG-cation

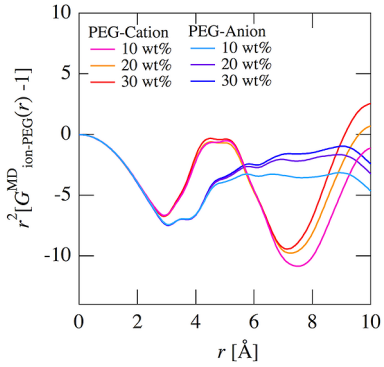

Figure 4. Partial radial distribution functions of PEG−cation and PEG−anion in 10, 20, and 30 wt % PEG/[C$_2$mIm$^+$][TFSA$^-$] solutions.

exhibited the first peak at around 4.2−5.2 Å for all the concentrations, while $G^{MD}_{PEG\text{-}an}(r)$ for PEG-anion did not have a significant peak at this r region and a board peaks appeared at r > 5 Å. This indicates that the PEG is preferentially solvated with C$_2$mIm cation rather than TFSA anion in the [C$_2$mIm$^+$]-[TFSA$^-$] solution.

Figure 5 shows the anion-type dependence on the partial $G^{MD}_{PEG\text{-}cat}(r)$ and $G^{MD}_{PEG\text{-}an}(r)$ obtained from 30 wt % PEG in

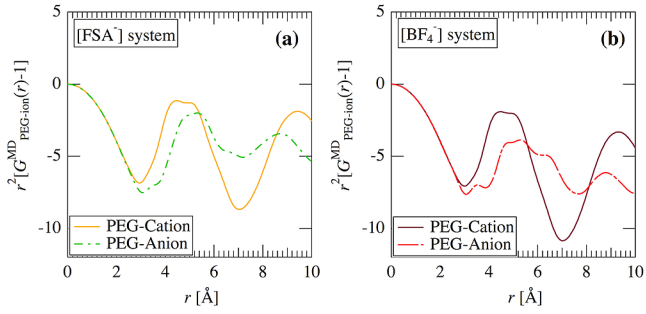

Figure 5. Anion-type dependence on the $r^2[G^{MD}_{PEG\text{-}ion}(r) - 1]$s for (a) [FSA$^-$] system and (b) [BF$_4^-$] system.

(a) [C$_2$mIm$^+$][FSA$^-$] and (b) [C$_2$mIm$^+$][BF$_4^-$] solution systems. It was found that the $G^{MD}_{PEG\text{-}cat}(r)$ exhibited the first peak at around 4.2−5.2 Å for FSA and BF$_4$ systems. On the other hand, the first peak in the $G^{MD}_{PEG\text{-}an}(r)$ appeared at around 5.5−6.0 Å for both systems. This suggests that the PEG prefers C$_2$mIm to anion even in FSA and BF$_4$ systems, which is similar to the TFSA system.

Figure 6 shows the spatial distribution functions (SDFs) for center of mass of [C$_2$mIm$^+$] cation (left) and [TFSA$^-$] anion (right) around oxygen atom of PEG chain end. In Figure S4, Supporting Information, the SDFs for FSA and BF$_4$ systems are also shown. The clouds in the SDF indicate the isoprobability surfaces of a given component (cation or anion) in three-dimensional box. It was found that the [C$_2$mIm$^+$] cation is directly coordinated to oxygen atoms of PEG and the orientation is high, while the anions distributed randomly. The SDF of cation around oxygen atom of PEG central position is also shown in Figure S5, Supporting Information,

dx.doi.org/10.1021/ma400218e | Macromolecules 2013, 46, 2369−2375

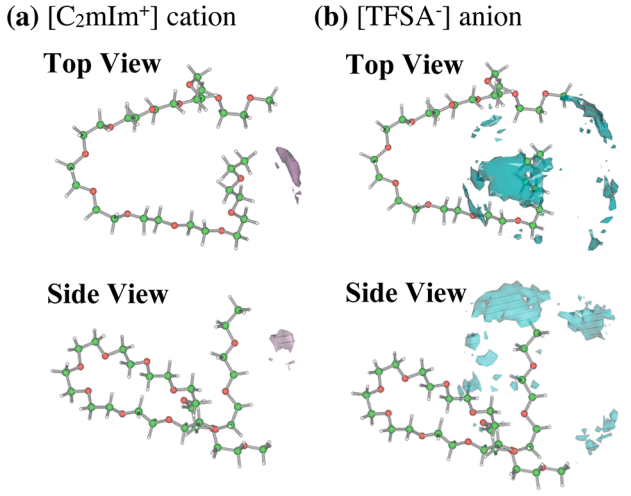

Figure 6. Spatial distribution functions (SDFs) of center of mass of (a) [C_2mIm^+] cation and (b) [$TFSA^-$] anion around the oxygen atom of a PEG chain end. The colored clouds indicate the isoprobability surfaces of a given ion. The red, green, white balls of PEG molecules represent the oxygen, carbon, and hydrogen atoms. The geometry of PEG set in the central position is one of equilibrium conformation obtained from MD simulations.

which shows no position dependence on the solvation of PEG by cation. This result suggests that interaction between cation and O atom (PEG) plays a key role on the solvation of PEG in IL. To discuss the PEG−cation interaction in detail, we calculated atom−atom pair correlation function, $g_{i\text{-}j}(r)$ with respect to PEG-cation interaction.

Figure 7 shows the atom−atom pair correlation functions, $g^{MD}{}_{Cn\text{-}O}(r)$s for C2, C4, and C5 positions of carbon of [C_2mIm^+] and oxygen atom of PEG chain, where $g^{MD}{}_{Cn\text{-}O}(r)$ is averaged among all the C*n*−O correlations. It was clearly found for all the IL systems that the C2 position is closest to PEG oxygen rather that C4 and C5 positions. The first peak in the $g^{MD}{}_{C2-O}(r)$ was at 3.3 Å for TFSA system, which is slightly shorter than those in the $g^{MD}{}_{C4-O}(r)$ and $g^{MD}{}_{C5-O}(r)$ at 3.4 and 3.4 Å, respectively. The $g^{MD}{}_{C2-O}(r)$ exhibited the first peak at 3.4 and 3.4 Å for FSA and BF_4 systems and those peak positions are also appreciably shorter than the corresponding peaks in the $g^{MD}{}_{C4-O}(r)$ and $g^{MD}{}_{C5-O}(r)$. Tsuda et al. pointed out from ^1H NMR study that hydrogen bonds are formed between C2 carbon of imidazolium cation and the O atom of PEG in IL solution.[11] Considering this result, we propose that the closer C2−O interaction mentioned above is originated from the hydrogen bond. The peak intensity of the first peak in the $g^{MD}{}_{C2-O}(r)$ was smaller than those of $g^{MD}{}_{C4-O}(r)$ and $g^{MD}{}_{C5-O}(r)$ for all the IL systems. This means that hydrogen bonding interaction for C2−O is minor for the solvation of PEG in IL, instead, the coulomb interactions of C4−O and C5−O are major interactions for the solvation of the ILs on PEG. Here, we note that the shape of the $g^{MD}{}_{Cn\text{-}O}(r)$ for TFSA system is similar to that for FSA system, while that for BF_4 system differs from both systems. In TFSA and FSA systems, the first peak in the $g^{MD}{}_{Cn\text{-}O}(r)$ is higher than the corresponding second peak at around 5.5 Å except for C2−O. This is because the molecular structure of TFSA is analogous to that of FSA. However, the reverse is observed in BF_4 system. Although it is not easy to explain this difference at the present stage, we point out here that the C*n* (cation) − O (PEG) interactions in the first coordination sphere in BF_4 system may be unfavorable compared with those in TFSA and FSA systems.

By integrating the $g^{MD}{}_{Cn\text{-}O}(r)$, we can evaluate the coordination number, *N* of C*n* carbon around O (PEG). In the case of TFSA system, the *N* in the first coordination sphere, i.e., the integration of the first peak in the $g^{MD}{}_{Cn\text{-}O}(r)$ from 0 to around 4 Å (valley between first and second peaks), was 0.81, 0.95, and 1.1 for C2, C4 and C5 position, respectively, resulting in the averaged $N = 0.96$. From the estimation of the averaged *N*, it was found that the averaged *N* decreases in the order of [$TFSA^-$] system (0.96) > [FSA^-] system (0.79) > [BF_4^-] system (0.60). Here, note that the anion size among them is in the order of [$TFSA^-$] > [FSA^-] > [BF_4^-]. In general, Coulombic interaction between cation and anion in the bulk IL is stronger for a smaller anion system, i.e., [C_2mIm^+][BF_4^-] > [C_2mIm^+][FSA^-] > [C_2mIm^+][$TFSA^-$]. In addition, it was found from our X-ray scattering and MD studies that specific hydrogen bonding interaction is formed evidently between cation and anion in [C_2mIm^+][BF_4^-] system relative to that in [C_2mIm^+][$TFSA^-$] system.[23,37,40] It is thus expected that solvation of PEG with IL ion easily occurs in [C_2mIm^+]-[$TFSA^-$] with a weaker cation−anion interaction in the bulk, because there is disruption of solvent−solvent interaction in the process of solvation. We can point out here that *N* depends on the strength of cation−anion interaction in the bulk IL.

Finally, let us discuss the relationship between the macroscopic and microscopic properties. It is expected that the microscopic properties in structural aspect such as anion size and the solvation number influence on the macroscopic swelling ratio and χ parameters shown in Table 1. As a matter

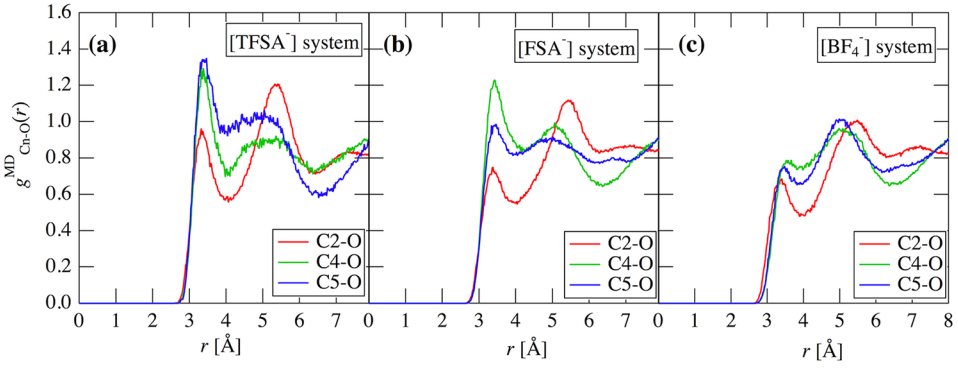

Figure 7. Atom-atom pair correlation functions $g^{MD}{}_{Cn\text{-}O}(r)$ between carbon of the cation and ether oxygen of PEG, for (a) [$TFSA^-$], (b) [FSA^-], and (c) [BF_4^-] systems. The $g^{MD}{}_{Cn\text{-}O}(r)$s are averaged among all the C*n* − O correlations.

dx.doi.org/10.1021/ma400218e | *Macromolecules* 2013, 46, 2369−2375

of fact, the swelling ratio of tetra-PEG gel becomes smaller by decreasing anion size ($[TFSA^-]$ > $[FSA^-]$ > $[BF_4^-]$ system), which is related to the extent of solvation of PEG. Indeed, the solvation number, N was evaluated to be in the order of $[TFSA^-]$ > $[FSA^-]$ > $[BF_4^-]$ system, as mentioned above. We thus point out here that the macroscopic properties of the ionic gel depending on the microscopic polymer solvation can be controlled by changing the solvent IL species, i.e., the ion−ion interaction in the bulk IL.

4. CONCLUSION

The solvation of PEG in ILs were directly evaluated as structural parameters, i.e., distance, orientation and coordination number, by using high-energy X-ray diffraction (HEXRD) experiments with the aid of molecular dynamics (MD) simulations. Dependences on the molecular weight (M_w), concentration and shape (linear or tetra-armed) of PEG and the composing anion species, X^- (= TFSA, FSA and BF_4) were investigated in the C_2mIm-based ionic liquids. From HEXRD experiments, it was found that there is no M_w dependence as well as the shape dependence for the PEG/$[C_2mIm^+][TFSA^-]$ solutions, indicating that the solvation structure at the local scale is not influenced by the M_w and shape of PEG. MD simulations for the PEG/IL solutions satisfactorily reproduced the HEXRD data. By combining the HEXRD with the MD results, it was found that the C_2mIm cation preferentially solvates to PEG and the anions distributed randomly for all the systems. From the atom−atom pair correlation function derived from MD result, we pointed out that the C2 position within C_2mIm cation interacts to PEG oxygen through hydrogen bond to give a high orientation of C2−O interaction. On the other hand, the corresponding C4 and C5 positions hardly form the hydrogen bond with PEG in the solution, but their interactions are major ones for the solvation to PEG, comparing with the hydrogen bond between C2−O. The macroscopic swelling ratio measurements were made on the PEG-based ion gel prepared from Tetra-PEG and the ILs examined in this work. It was concluded that the swelling ratio decreases in the same order of the anion size and solvation number. We thus proposed that the macroscopic properties such as swelling ratio and χ parameter are strongly related to the microscopic solvation of polymer.

■ ASSOCIATED CONTENT

Ⓢ Supporting Information

Composition and densities of the systems for the MD simulation, $S^{exp}(q)$s and $r^2[G^{exp}(r) - 1]$s for PEG/$[C_2mIm^+][TFSA^-]$ solutions (all the experimental data), M_w dependence of $S^{exp}(q)$s and $G^{exp}(r)$s for 20 wt % PEG in $[C_2mIm^+][TFSA^-]$ solutions, inter- and intramolecular $G^{MD}(r)$s for 30 wt % PEG/$[C_2mIm^+][TFSA^-]$, SDFs for $[C_2mIm^+][FSA^-]$ and $[C_2mIm^+][BF_4^-]$ systems, and SDFs for $[C_2mIm^+][TFSA^-]$ system around the middle of a PEG chain are shown in Table S1 and Figure S1, S2, S3, S4, and S5, respectively. These materials are available free of charge via the Internet at http://pubs.acs.org.

■ AUTHOR INFORMATION

Corresponding Author

*E-mail: (K.F.) k-fujii@issp.u-tokyo.ac.jp.

Notes

The authors declare no competing financial interest.

■ ACKNOWLEDGMENTS

This work has been financially supported by Grant-in-Aids for Scientific Research from the Ministry of Education, Culture, Sports, Science and Technology (No. 24750066 to K.F., No. 22245018 to M.S.). The synchrotron radiation experiments were performed at the BL04B2 of SPring-8 with the approval of the Japan Synchrotron Radiation Research Institute (JASRI) (Proposal No. 2012A1561).

■ REFERENCES

(1) Welton, T. *Chem. Rev.* **1999**, *99*, 2071−2083.
(2) Buzzeo, M. C.; Evans, R. G.; Compton, R. G. *Chem. Phys. Chem.* **2004**, *5*, 1106−1120.
(3) Galinski, M.; Lewandowski, A.; Stepniak, I. *Electrochim. Acta* **2006**, *51*, 5567−5580.
(4) Armand, M.; Endres, F.; MacFarlane, D. R.; Ohno, H.; Scrosati, B. *Nature Mater.* **2009**, *8*, 621−629.
(5) Chiappe, C.; Pieraccini, D. *J. Phys. Org. Chem.* **2005**, *18*, 275−297.
(6) Wasserscheid, P.; Keim, K. *Angew. Chem., Int. Ed.* **2000**, *39*, 3772−3789.
(7) Winterton, N. *J. Mater. Chem.* **2006**, *16*, 4281.
(8) Swatloski, R. P.; Spear, S. K.; Holbrey, J. D.; Rogers, R. D. *J. Am. Chem. Soc.* **2002**, *124*, 4974−4975.
(9) Fukaya, Y.; Hayashi, K.; Wada, M.; Ohno, H. *Green Chem.* **2008**, *10*, 44−46.
(10) Abe, M.; Fukaya, Y.; Ohno, H. *Green Chem.* **2010**, *12*, 1274−1280.
(11) Tsuda, R.; Kodama, K.; Ueki, T.; Kokubo, H.; Imabayashi, S.; Watanabe, M. *Chem. Commun.* **2008**, 4939.
(12) Lee, H. N.; Newell, N.; Bai, Z.; Lodge, T. P. *Macromolecules* **2012**, *45*, 3627−3633.
(13) Costa, L. T.; Riberio, M. C. C. *J. Chem. Phys.* **2006**, *124*, 184902.
(14) Matsugami, M.; Fujii, K.; Ueki, T.; Kitazawa, Y.; Umebayashi, Y.; Watanabe, M.; Shibayama, M. *Anal. Sci.* **2013**, *29*, 311.
(15) Fujii, K.; Ueki, T.; Niitsuma, K.; Matsunaga, T.; Watanabe, M.; Shibayama, M. *Polymer* **2011**, *52*, 1589−1595.
(16) Fukushima, T.; Asaka, K.; Kosaka, A.; Aida, T. *Angew. Chem., Int. Ed.* **2005**, *44* (16), 2410−2413.
(17) Takeuchi, I.; Asaka, K.; Kiyohara, K.; Sugino, T.; Terasawa, N.; Mukai, K.; Fukushima, T.; Aida, T. *Electrochim. Acta* **2009**, *54* (6), 1762−1768.
(18) Bara, J. E.; Carlisle, T. K.; Gabriel, C. J.; Camper, D.; Finotello, A.; Gin, D. L.; Noble, R. D. *Ind. Eng. Chem. Res.* **2009**, *48* (6), 2739−2751.
(19) Fujii, K.; Asai, H.; Ueki, T.; Sakai, T.; Imaizumi, S.; Chung, U.; Watanabe, M.; Shibayama, M. *Soft Matter* **2012**, *8* (6), 1756−1759.
(20) Asai, H.; Fujii, K.; Ueki, T.; Sakai, T.; Chung, U.; Watanabe, M.; Han, Y. S.; Kim, T. H.; Shibayama, M. *Macromolecules* **2012**, *45*, 3902−3909.
(21) Asai, H.; Nishi, K.; Hiroi, T.; Fujii, K.; Sakai, T.; Shibayama, M. *Polymer* **2013**, *54*, 1160−1166.
(22) Fujii, K.; Nonaka, T.; Akimoto, Y.; Umebayashi, Y.; Ishiguro, S. *Anal. Sci.* **2008**, *24*, 1377−1380.
(23) Fujii, K.; Kanzaki, R.; Takamuku, T.; Kameda, Y.; Kohara, S.; Kanakubo, M.; Shibayama, M.; Ishiguro, S.; Umebayashi, Y. *J. Chem. Phys.* **2011**, *135*, 244502.
(24) Kohara, S.; Suzuya, K.; Kashihara, Y.; Matsumoto, N.; Umesaki, N.; Sakai, I. *Nucl. Instrum. Meth. A* **2001**, *467−468*, 1030.
(25) Isshiki, M.; Ohishi, Y.; Goto, S.; Takeshita, K.; Oshikawa, T. *Nucl. Instrum. Meth. A* **2001**, *467−468*, 663.
(26) Sasaki, S. *KEK Report*; National Laboratory for High Energy Physics: Tsukuba, Japan, 1991; Vol. *90−16*.
(27) Cromer, D. T. *J. Chem. Phys.* **1969**, *50*, 4857.
(28) Hubbell, J. H.; Veigele, W. J.; Briggs, E. A.; Brown, R. T.; Cromer, D. T.; Howerton, R. J. *J. Phys. Chem. Ref. Data* **1975**, *4*, 471−493.
(29) Cromer, D. T.; Mann, J. B. *J. Chem. Phys.* **1967**, *47*, 1892−1893.

(30) Maslen, E. N.; Fox, A. G.; O'Keefe, M. A. *International Tables for Crystallography*; Kluwer: Dordrecht, The Netherlands, 1999; Vol. C, p 572.
(31) Lopes, J. N. A. C.; Pádua, A. A. H. *J. Phys. Chem. B* **2004**, *108*, 2038−2047.
(32) Lopes, J. N. A. C.; Pádua, A. A. H. *J. Phys. Chem. B* **2006**, *110*, 19586−19592.
(33) Cornell, W. D.; Cieplak, P.; Bayly, C. I.; Gould, I. R.; Merz, K. M.; Ferguson, D. M.; Spellmeyer, D. C.; Fox, T.; Caldwell, J. W.; Kollman, P. A. *J. Am. Chem. Soc.* **1995**, *117*, 5179−5197.
(34) Fujii, K.; Mitsugi, T.; Takamuku, T.; Yamaguchi, T.; Umebayashi, Y.; Ishiguro, S. *Chem. Lett.* **2009**, *38*, 340−341.
(35) Umebayashi, Y.; Hamano, H.; Tsuzuki, S.; Lopes, J. N. A. C.; Pádua, A. A. H.; Kameda, Y.; Kohara, S.; Yamaguchi, T.; Fujii, K.; Ishiguro, S. *J. Phys. Chem. B* **2010**, *114*, 11715−11724.
(36) Fukuda, S.; Takeuchi, M.; Fujii, K.; Kanzaki, R.; Takamuku, T.; Chiba, K.; Yamamoto, H.; Umebayashi, Y.; Ishiguro, S. *J. Mol. Liq.* **2008**, *143*, 2−7.
(37) Fujii, K.; Soejima, Y.; Kyoshoin, Y.; Fukuda, S.; Kanzaki, R.; Umebayashi, Y.; Yamaguchi, T.; Ishiguro, S.; Takamuku, T. *J. Phys. Chem. B* **2008**, *112*, 4329.
(38) Kanzaki, R.; Mitsugi, T.; Fukuda, S.; Fujii, K.; Takeuchi, M.; Soejima, Y.; Takamuku, T.; Yamaguchi, T.; Umebayashi, Y.; Ishiguro, S. *J. Mol. Liq.* **2009**, *147*, 77.
(39) Fujii, K.; Seki, S.; Fukuda, S.; Takamuku, T.; Kohara, S.; Kameda, Y.; Umebayashi, Y.; Ishiguro, S. *J. Mol. Liq.* **2008**, *143*, 64−69.
(40) Umebayashi, Y.; Chung, W.-L.; Mitsugi, T.; Fukuda, S.; Takeuchi, M.; Fujii, K.; Takamuku, T.; Kanzaki, R.; Ishiguro, S. *J. Comput. Chem. Jpn.* **2008**, *7*, 125−134.
(41) Flory, P. J.; Rehner, J., Jr. *J. Chem. Phys.* **1943**, *11*, 521−526.
(42) Matsunaga, T.; Sakai, T.; Akagi, Y.; Chung, U.; Shibayama, M. *Macromolecules* **2009**, *42* (4), 1344−1351.
(43) Flory, P. J., *Principles of Polymer Chemistry*; Cornell Univ.: Ithaca, NY, 1953.
(44) Umebayashi, Y.; Hamano, H.; Seki, S.; Minofar, B.; Fujii, K.; Hayamizu, K.; Tsuzuki, S.; Kameda, Y.; Kohara, S.; Watanabe, M. *J. Phys. Chem. B* **2011**, *115*, 12179−12191.